Isothermal Switching and Detailed Filament Evolution in Memristive Systems

Patrick R. Mickel, Andrew J. Lohn, Conrad D. James, and Matthew J Marinella*

Filamentary memristive systems,[1–3] which tune their resistance state through the modification of nanoscale conduction channels, are leading candidates for the future of digital memory storage[4–6] and are believed to enable entirely new approaches to circuitry and computation.[5,6] Accordingly, to realize this technological potential, understanding the physical mechanisms which govern memristive switching has become a field of intense research.[2,7–10] However, due to the limited contrast between the filament and its environment and because these phenomena occur at virtually inaccessible lengths scales, characterizations have required formidable experimental effort,[11–13] limiting physical understanding. Transmission electron microscopy studies are the de facto characterization technique,[3,9,12,13] yet they typically provide only a single post-mortem filament state snapshot. Furthermore, despite its fundamental importance,[8,10,14–16] filament temperature evolution is all but unknown experimentally. Here, we demonstrate that filamentary resistive switching is an isothermal process, and we present and experimentally validate a set of constitutive equations which provide the steady-state solution for filamentary resistive switching. We show that the application of these equations to a single hysteresis loop provides a continuous and quantitatively accurate description of the evolution of the filament radius, composition, heat flow, and temperature across the entire resistive switching range. Furthermore, we show that this steady-state solution applies to a large range of filamentary metal oxide RRAM switching materials, and over almost all experimentally relevant time-scales.

Canonical memristive systems, as predicted by Chua,[17,18] modify their resistance state according to the history of applied voltage flux, resulting in smoothly varying, pinched current-voltage (IV) hysteresis loops (see inset of **Figure 1**a). However, memristors based on nanoscale conducting filaments seldom display this canonical curvature. Thermal activation is widely believed to be central to resistive switching,[15,16] and the onset of switching may be interpreted as the activation of drift/diffusion by Joule heating. Decreasing voltage would thereby lower temperature below T_{crit}, freezing the resistance state, and explaining the experimentally observed sharp IV end-points (circled points in Figure 1a and b) which are absent in classical memristor theory (Figure 1a inset).

P. R. Mickel,[+] A. J. Lohn,[+] C. D. James, M. J Marinella
Sandia National Laboratories
Albuquerque, New Mexico
E-mail: prmicke@sandia.gov
[+]These authors contributed equally to this work.

DOI: 10.1002/adma.201306182

Even more intriguing is that these sharp IV end-points exist at all points throughout resistive switching. Figure 1a shows hysteresis curves measured on TaO_x memristors where the resistive switching was current-limited for ON switching and voltage-limited for OFF switching (fabrication details have been previously reported[19,20]). The different IV end-points apply significantly different Joule heat doses, however, each switching curve exhibits equally sharp transitions, strongly implying that $T \approx T_{crit}$ at each switching point, and that the resistive switching is an isothermal process. This suggests the presence of an unidentified negative feedback mechanism that balances the system near the thermal activation threshold.

To investigate this negative feedback process, we developed a simple heat flow model of a filamentary resistive switching device. In steady state, Joule heat (Q_{tot}, or IV) is generated uniformly in a cylindrical filament and flows out both vertically (Q_z) through the electrodes and radially (Q_r) through its surroundings (see **Figure 2**a). Comparing the total Joule heat generation to the vertical heat flow allows determination of the radial filament surface temperature, T_S (see Supporting Information for derivation):

$$T_S = T_{RT} + \sigma V^2 \frac{d_E}{2k_E d_O}\left[1 - \frac{k_E}{k_F}\frac{r_F^2}{4d_E d_O}\right] \quad (1)$$

where T_{RT} is room temperature, σ is electrical conductivity, V is voltage, d_E is electrode thickness, k_E is electrode thermal conductivity, d_O is thickness of the oxide insulator, r_F is filament radius, and k_F is filament thermal conductivity.

Recent experimental evidence has suggested that resistive switching is mediated by filament radius modulations.[1,2,10] Considering this, the negative sign in Equation (1) reveals the temperature limiting mechanism for ON switching (lowering resistance) – temperature decreases with increasing filament radius. This occurs due to the fact that core temperatures increase with radius and $Q_z \propto T$. Thus, Q_z increases with radius faster than heat generation and Q_r (and as a result, T_S) therefore decreases, freezing ion motion at a radius determined by the applied power.

OFF switching (increasing resistance) produces similarly sharp, non-Chuan IV end-points (see circled points in Figure 1b), again suggesting that feedback balances the system at the edge of activation, resulting in isothermal switching. Considering Equation (1), this experimental observation rules out filament radius changes as an OFF switching mechanism. Decreasing r_F increases temperature, resulting in positive feedback which would amplify rather than self-limit filament temperature. It is highly unlikely that parameters such as the electrode or oxide thickness change substantially and reversibly

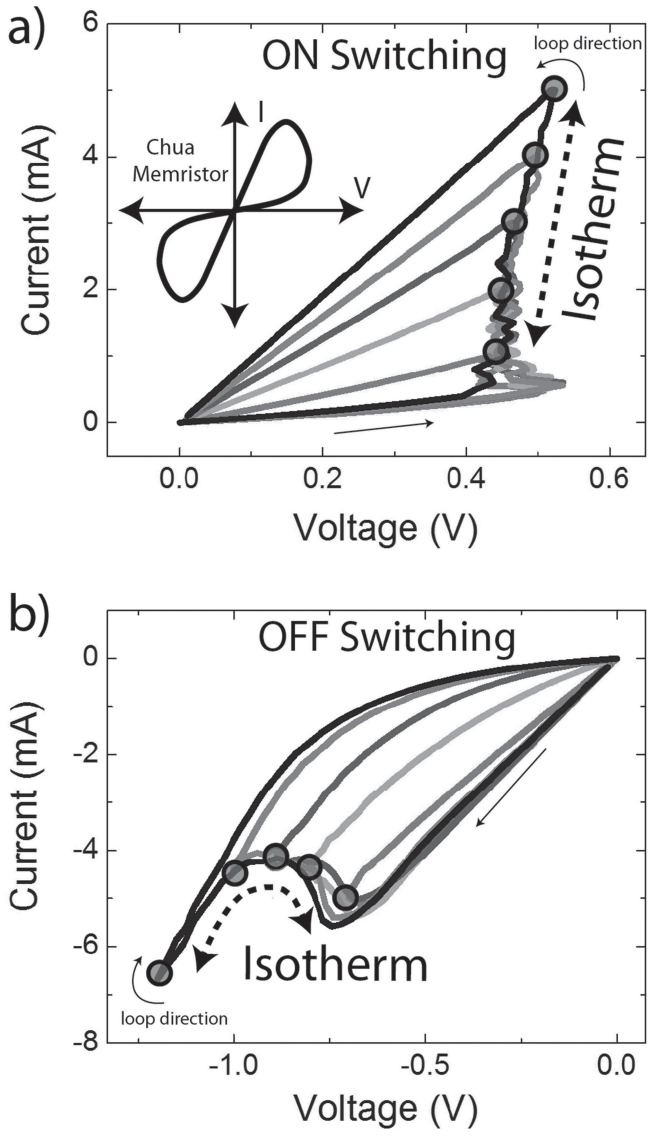

Figure 1. ON and OFF switching hysteresis curves show evidence of isothermal switching. a) Multiple current sourced ON switching curves with varying maximum current are shown. The sharp termination of switching with a decrease in current suggests the system is near a thermally activating temperature. The multiple hysteresis curves show that all switching points share the sharp termination, suggesting that all switching points share a common temperature (i.e. isothermal switching). Inset: a comparison to canonical Chua memristors is shown, highlighting the smooth endpoints, and the absence of the experimentally observed non-perturbative voltage sweep range. b) Multiple voltage sourced OFF switching loops are shown, suggesting that OFF switching is also isothermal.

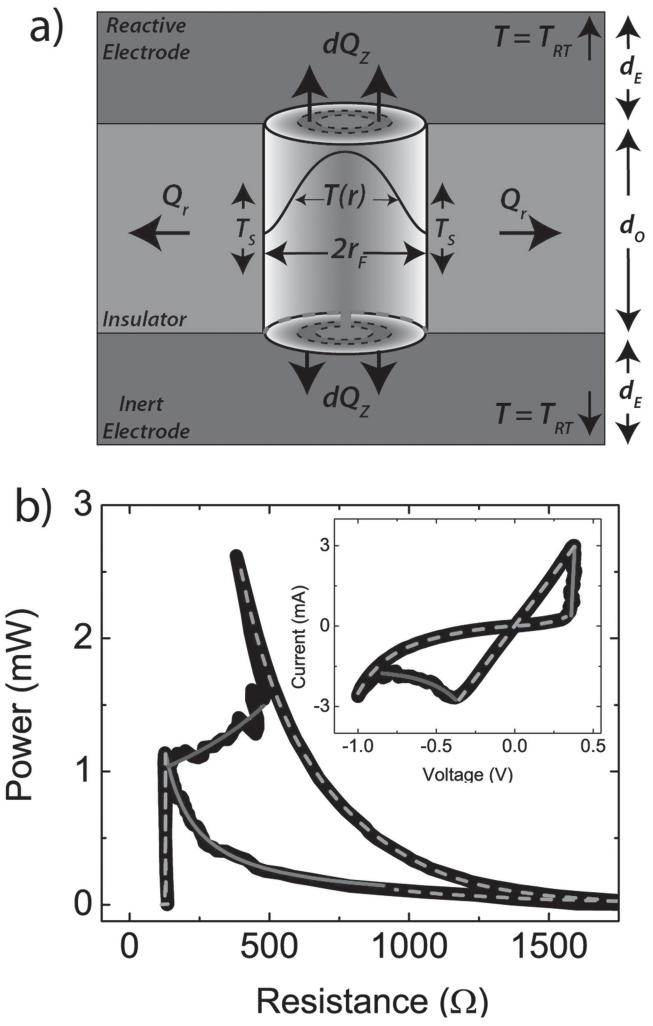

Figure 2. Thermal model geometry and a comparison to resistive switching data. a) A schematic illustration of the heat flow associated with a conducting filament of radius r_F and uniform conductivity (or equivalently, oxygen vacancy concentration) in an insulating environment is shown. Heat flow is decomposed into two components: Q_r and Q_z, with $Q_{Tot} = Q_r + Q_z$. The temperature profile within the filament, $T(r)$, results in a spatially varying local $\hat{z}$ heat flow, dQ_z, while the constant surface temperature, T_S, results in a constant radial heat flow, Q_r. T_S is the temperature which remains constant during the isothermal switching depicted in Figure 1. d_o and d_E are the oxide and electrode thicknesses, respectively. As shown, the boundary conditions assume the outer edge of the electrodes are held constant at room temperature, T_{RT}. b) The experimental and theoretically calculated hysteresis loops are shown in two coordinate systems: (1) the typical current-voltage basis, and (2) the power-resistance basis natural to the constitutive equations derived here. The loops are divided into four portions: ON switching (red, Equation (2a), ON state (green, Ohmic conduction), OFF switching (blue, Equation (2b), and OFF state (orange, Ohmic and Poole-Frenkel conduction). The fitting parameters for the switching curves were: $T_{crit} = 1650$ K, $k_E = 145.3$ W m^{-1} K^{-1}, and $\sigma_{max} = 6.25e5\ \Omega^{-1}m^{-1}$. The OFF state is modeled according to the equation: $I(V) = V(a + be^{c\sqrt{V}})$, where 1/a = 1.5 kΩ, 1/b = 1.33 MΩ, and c = 7.8 V$^{-1/2}$. ON and OFF state fits are shown in dashed lines, as they are not predicted by the switching model discussed in this work.

during switching, therefore, Equation (1) suggests that decreases in conductivity provide the self-regulation of temperature for OFF switching. Importantly, this suggests that bipolar operation is primarily driven by changes in two independent state variables (radius and conductivity).

To validate these hypotheses, we must demonstrate that the filament surface temperature (T_S) decreases with increasing radius and decreasing conductivity, resulting in a constant switching temperature. This is a daunting task, as few (if any) experimental methods can measure the temperature of a nanoscale filament, and TEM imaging typically provides only a snapshot of filament geometry and composition. However,

Adv. Mater. 2014,
DOI: 10.1002/adma.201306182

assuming isothermal switching and setting $T_S = T_{crit}$ (assuming all switching occurs with a constant/isothermal radial surface temperature equal to the critical activating temperature), Equation (1) may be rewritten as a set of constitutive equations defining the system's response to power dissipation (see Supporting Information for derivation):

$$IV_r = A_r \frac{T_{crit} - T_{RT}}{R - R_{min}} \tag{2a}$$

$$IV_\sigma = A_\sigma \frac{T_{crit} - T_{RT}}{R_{max} - R} \tag{2b}$$

where $R_{min} = \frac{k_E}{4\pi\sigma_{max}^2 L_{WF} T_{crit} d_E}$, $A_r = \frac{2k_E d_O}{\sigma_{max} d_E}$, $R_{max} = \frac{4d_O^2 L_{WF} T_{crit} d_E}{\pi r_{max}^4 k_E}$, $A_\sigma = \frac{8d_O^2 L_{WF} T_{crit}}{r_{max}^2}$, r_{max} is the maximum previous filament radius, σ_{max} is the saturation conductivity of the ON state, and L_{WF} is the Wiedemann-Franz constant. The subscripts r and σ in Equation (2a) denote which variable is allowed to change in Equation (1), and can roughly be interpreted here as ON and OFF switching, respectively. Comparing these equations to resistive switching data provides a direct test of both the isothermal assumption as well as the predicted state variables for both ON and OFF switching (radius and conductivity, respectively)

Figure 2b compares memristive switching data with Eqs. 2, demonstrating strong agreement between theory and experiment with the use of only three physical fitting parameters: T_{crit}, k_E, and σ_{max} (r_F is determined via $R = d_O/\sigma\pi r_F^2$ during ON switching). In fitting the curves, a single $T_{crit}, \sigma_{max}, k_E$ combination is determined which is consistence with all switching points, therefore demonstrating that the isothermal assumption is accurate across the continuum of resistance values. Only a single hysteresis loop is shown, however, the model has successfully described a diverse set of fabricated devices, with varying device structures, oxide thicknesses (5–15 nm), electrode materials (Ta, Pt, TiN), growth chambers and targets, and areas (100 um to 350 nm). The physical fitting parameters had quite reasonable ranges over our set of test devices: 8.5 nm r_{max} 13.2 nm and $7.2 \times 10^4\ \Omega^{-1}\text{m}^{-1} < \sigma_{max} < 8.3 \times 10^5\ \Omega^{-1}\text{m}^{-1}$ are consistent with the range of previous reports,[11] $T_{crit} \approx$ 1300 K -1700 K is in close agreement with finite element thermal modeling[14,16] and is consistent with the observation of nanocrystalline Ta_2O_5 near formed filaments[12] ($T_{crystallization} \approx$ 1633K), and 89 W $\text{m}^{-1}\text{K}^{-1}$ $k_E <$ 200 W $\text{m}^{-1}\text{K}^{-1}$, which considering the expected overestimation due to the assumed cylindrical electrode geometry is in good agreement with the expected value for the device electrodes (see the Supporting Information for the curve fits corresponding to these fitting parameters). Additionally, the prediction of R_{min} is in quantitative agreement with previous reports.[21]

Here, r_{max} and σ_{max} represent the maximum radius and conductivity throughout switching. However, r_F and σ are free to vary during ON and OFF switching, respectively. Therefore, combining Eqs. 2 with the known cylindrical resistance, $R = d_O/\sigma\pi r_F^2$, provides a continuous description of the evolution of each of these parameters throughout the entire switching range (i.e. Equation (2a) implicitly describes multi-level resistance state setting: by choosing a SET or RESET power, any analog resistance value may be programmed). Importantly, it should be emphasized that continuous characterizations of these parameters were previously prohibitively difficult (r, σ)[11,12] if not experimentally impossible (T, k_E).[14,16] In fact, successful in-situ characterization of filament geometry and composition during switching has only very recently been accomplished.[22,23] In contrast, Equation (2a) provides a complete filament characterization using a single hysteresis curve. Additionally, it should be noted that the thermal conductivity reported for the electrodes is in fact an effective term which may take into account the thermal resistance of the entire vertical surrounding and could include effects from inter-layer dielectrics, substrates, and vias. However, as the total thermal resistance is in fact the most important factor, we view this as a strength rather than limitation of the model.

Surprisingly, assuming the presence of bipolar motion due to drift and specifying when it is thermally allowed is all that is necessary to describe the state evolution, and circumvents specifying additional complex microscopic mechanisms. However, a qualitative physical depiction is still beneficial, and is presented in **Figure 3** for multiple switching regimes. During ON switching, vacancies first flow in the hot center of a previously electroformed region and "pile-up" due to the low solubility of O^{2-} in an inert electrode (Figure 3a). This process continues until a core filament reaches a uniform oxygen vacancy saturation concentration. Next, the vacancies flow toward the outer edges of the filament where the concentration is sub-saturation (Figure 3b). This process continues until the temperature falls below activation or the power required for continued switching diverges as the radius increases, causing $R \to R_{min}$ ($P \to \infty$, per Equation (2a)). During OFF switching, vacancy saturation no longer limits ion motion, and the filament is quasi-uniformly depleted as vacancies leave vertically without replacement from the inert electrode (Figure 3c). The effective conductivity decreases until the temperature falls below activation or all vacancies have left and $R \to R_{max}$. The depletion is described as 'quasi-uniform' because vacancies will leave the center of the filament where T_{crit} is reached first, possibly leading to filament ruptures as predicted by Larentis et al[10] (a discussion of when filament ruptures occur during OFF switching is provided in the Supporting Information). Prior to rupture, current is subsequently diverted from these regions, self-limiting their thermal activation and leading to depletion in neighboring regions (Equation (2b) applies most accurately once this process has stabilized). Finally, because OFF states are experimentally less resistive than virgin devices, it is highly likely that some permanent oxygen vacancy locations remain (Figure 3d).

Figure 4a shows the reproduction of an empirical approximation,[24] $R = V_{set}/I_C$ (where I_C is the compliance current, and V_{set} is held constant at 0.4 V), which was shown to approximate resistive switching events in a large range of materials[24]: HfO_X,[24] TiO_X,[25] ZrO_X,[26] and TaO_X. Also shown is a fit to the constitutive equation presented here (Equation (2a)). The constitutive equation reproduces the empirical trend at high resistance and shows improved agreement at lower resistance. The departure from the empirical fit at low resistance results from the breakdown of the constant voltage approximation in that range. Since Equation (2a) analytically determines the set voltage, this departure is accurately predicted and can be physically understood. Reproduction of the empirical relation and

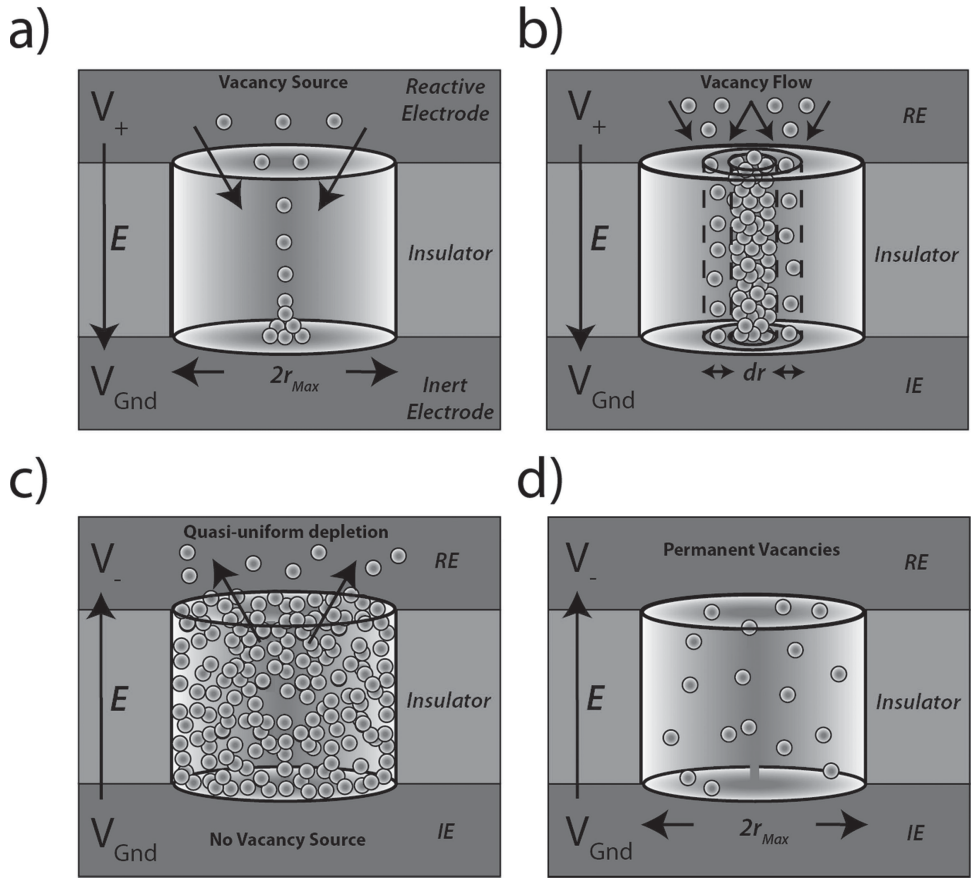

Figure 3. Schematic depicting microscopic ionic flux during switching. a) During ON switching (V_+ on top electrode) vacancies first flow in the hot filament center and "pile-up" at the bottom electrode interface due to the insolubility of O^{2-} in inert electrodes. b) Once the filament has reached a uniform oxygen vacancy saturation concentration, additional oxygen vacancy flux acts to increase the filament radius. c) During OFF switching (V_- on top electrode), vacancy saturation no longer limits ion motion, and because Pt has no reservoir of vacancies, the filament is quasi-uniformly depleted. d) After oxygen vacancy depletion has completed, some permanent vacancy locations remain. In our specific devices, the reactive electrodes are tantalum, and the inert electrodes are platinum.

the agreement with multiple switching materials suggests a universal applicability of Eqs. 2 to a wide range of filamentary resistive switches.

The constitutive equations derived here assume a time-independent temperature during switching, and therefore only describe resistive switching which occurs slower than thermal steady-state. Figure 4b compares 10 ns switching data digitized from Ref. [27] with fits to Equation (2a), demonstrating strong quantitative agreement, and suggesting thermal steady-state is achieved at sub-nanosecond time-scales.[27] This result is supported by a simple heat flow dynamics model:

$$\dot{Q}_{gen} = N_F C_F \frac{dT_F}{dt} + N_E C_E \frac{dT_E}{dt} + dG_{T,z} A (T_F - T_{RT}) \quad (3)$$

where $\dot{Q}_{gen}$ is the Joule heat generation, N_F is the number of moles of the filament material, C_F is the molar heat capacity of TaO_x, N_E is the number of moles of the electrode material, C_E is the molar heat capacity of Ta, $\frac{dT}{dt}$ is the time derivative of temperature, $dG_{T,z}$ is the $\hat{z}$ interfacial thermal conductance (measured directly by fits to Equation (2a)), and $A = \pi r_F^2$ is the cross-sectional filament area. Setting $T_E = \frac{1}{2} T_F$ (assuming a linear temperature gradient the average electrode temperature is roughly half of T_E), Equation (3) determines the time required for the filament to reach an activating temperature of $T_{crit} \approx 1500$ K. As shown in the inset of Figure 4b, Equation (3) suggests quite rapid heating, as filaments as large as 10 nm require less than 100 ps to activate.

In conclusion, we derived and experimentally verified a set of constitutive equations that govern steady state filamentary memristive switching. These equations identified and explained the self-limiting thermal physics which controls both ON and OFF filamentary switching. We demonstrated that applying these equations to a single hysteresis loop allows any researcher with a voltage/current sourcemeter to characterize the internal structure and evolution of the conducting filament throughout the entire switching process, with a continuous description of its: composition, radius, surrounding thermal resistance, and temperature. Additionally, the analytical nature of the solution provides a compact and efficient method to explore device performance dependencies on design parameters. And finally, these steady-state constitutive equations were shown to apply to a large range of filamentary resistive switching materials, and over almost all technologically/experimentally relevant time-scales.

Adv. Mater. 2014,
DOI: 10.1002/adma.201306182

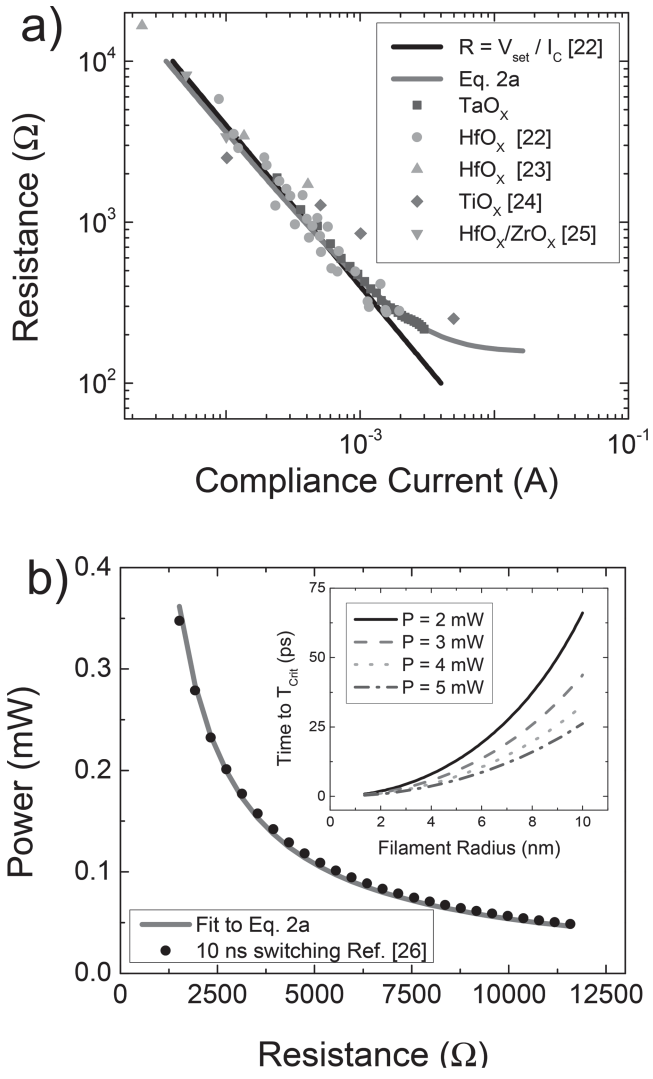

Figure 4. Comparison to other materials and time-scales. a) Equation (2a) is compared to a broad range of resistive switching materials as well as the suggested empirical relation, $R = V_{set}/I_C$ introduced in Ref. [24] where $V_{set} \approx 0.4$ V and I_C is the compliance current. Equation (2a) is shown to recover this result and generalize it to the low resistance regime, where V_{set} departs from a constant value. b) High speed switching data from Ref. [27] is compared to Equation (2a). The strong agreement suggests that thermal steady state exists at the nano-second time-scale, and that Equation (2) is relevant at small time-scales. Inset: The time necessary for the system to heat to T_{crit} is calculated according to Equation (3) for multiple applied powers, suggesting that activating temperatures may be reached for most filament sizes in less than 100 ps.

Supporting Information

Supporting information is available from the Wiley Online Library or from the author.

Acknowledgements

We would like to acknowledge James E. Stevens and the Sandia MESA Fab for device fabrication. We also like to thank Robert M. Fleming and Edward I. Cole for their valuable feedback. We also like to acknowledge J.J. Yang and R.S. Williams for providing additional test samples and valuable discussions. This work was funded by Sandia's Laboratory Directed Research and Development program. Sandia National Laboratories is a multi-program laboratory managed and operated by Sandia Corporation, a wholly owned subsidiary of Lockheed Martin Corporation, for the U.S. Department of Energy's National Nuclear Security Administration under contract DE-AC04–94AL85000.

Received: December 18, 2013
Revised: March 24, 2014
Published online:

[1] J. J. Yang, D. B. Strukov, D. Stewart. *Nat. Nano.* **2013**, *8*, 13–24,
[2] R. Waser, R. Dittmann, G. Staikov, K. Szot, *Adv. Mater.* **2009**, *21*, 2632–2663.
[3] R. Waser, M. Aono, *Nat. Mater.* **2007**, *6*, 833–840.
[4] G. W. Burr, B. N. Kurdi, J. C. Scott, C. H. Lam, K. Gopalakrishnan, R. S. Shenoy, *IBM J. Research and Development* **2008**, *52*, 449–464.
[5] M. D. Pickett, G. Medeiros-Ribeiro, R. S. Williams, *Nat. Mater.* **2013**, *12*, 114–117.
[6] S. H. Jo, T. Chang, I. Ebong, B. B. Bhadviya, P. Mazumder, W. Lu, *Nano Letters* **2010**, *10*, 1297–1301.
[7] D. B. Strukov, G. S. Snider, D. R. Stewart, R. S. Williams, *Nature* **2008**, *453*, 80–83.
[8] P. R. Mickel, A. J. Lohn, B. J. Choi, J. J. Yang, M. X. Zhang, M. J. Marinella, R. S. Williams, *Appl. Phys. Lett.* **2013**, *102*, 223502.
[9] M. Lee, C. B. Lee, D. Lee, S. R. Lee, M. Chang, J. H. Hur, Y. Kim, C. Kim, D. H. Seo, S. Seo, U. Chung, I. Yoo, K. Kim, *Nat. Mater.* **2011**, *10*, 625–630.
[10] S. Larentis, F. Nardi, S. Balatti, D. C. Gilmer, D. Ielmini, *Electron Devices, IEEE Transactions on* **2012**, *59*, 2468–2475.
[11] F. Miao, W. Yi, I. Goldfarb, J. J. Yang, M. Zhang, M. D. Pickett, J. P. Strachan, G. Medeiros-Ribeiro, R. S. Williams, *ACS Nano* **2012**, *6*, 2312–2318.
[12] F. Miao, J. P. Strachan, J. J. Yang, M. Zhang, I. Goldfarb, A. C. Torrezan, P. Eschbach, R. D. Kelley, G. Medeiros-Ribeiro, R. S. Williams, *Adv. Mater.* **2011**, *23*, 5633–5640.
[13] D.-H. Kwon, K. M. Kim, J. H. Jang, J. M. Jeon, M. H. Lee, G. H. Kim, X. Li, G. Park, B. Lee, S. Han, *Nat. Nano.* **2010**, *5*, 148–153.
[14] D. B. Strukov, F. Alibart, R. S. Williams, *Appl. Phys. A* **2012**, *107*, 509–518.
[15] D. Strukov, R. S. Williams, *Appl. Phys. A* **2009**, *94*, 515–519.
[16] S. Larentis, C. Cagli, F. Nardi, D. Ielmini, *Microelectron. Eng.* **2011**, *88*, 1119–1123.
[17] L. Chua, *Circuit Theory, IEEE Transactions on* **1971**, *18*, 507–519.
[18] L. O. Chua, K. Sung Mo, *Proc. IEEE* **1976**, *64*, 209–223.
[19] A. J. Lohn, J. E. Stevens, P. R. Mickel, Hughart, D. R. Marinella, *ECS Transactions* **2013**, *58*, 59–65.
[20] A. J. Lohn, J. E. Stevens, P. R. Mickel, M. J. Marinella, *Appl. Phys. Lett.* **2013**, *103*, 063502.
[21] A. J. Lohn, P. R. Mickel, M. J. Marinella, **2013**, *103*, 173503.
[22] G.-S. Park, Y. B. Kim, S. Y. Park, X. S. Li, S. Heo, M. Lee, M. Chang, J. H. Kwon, M. Kim, U. Chung, R. Dittmann, R. Waser, K. Kim, *Nat. Commun. 4*, **2013**, doi:10.1038/ncomms3382.
[23] J.-Y. Chen, C. Hsin, C. Huang, C. Chiu, Y. Huang, S. Lin, W. Wu, L. Chen, *Nano Lett.* **2013**, *13*, 3671–3677.
[24] D. Ielmini, F. Nardi, S. Balatti, *Electron Devices, IEEE Transactions on* **2012**, *59*, 2049–2056.
[25] J. Park, J. Park, S. Jung, S. J. Lee, J. W. Lee, W. S. Kim, S. J. Shin, H. Hwang, *Microelectron. Eng.* **2011**, *88*, 1136–1139.
[26] L. Joonmyoung, *Electron Devices Meeting (IEDM), 2010 IEEE International*. 19.15.11–19.15.14.
[27] J. P. Strachan, A. C. Torrezan, G. Medeiros-Ribeiro, R. S. Williams, *Nanotechnology* **2011**, *22*, 505402.